JOURNAL OF VIROLOGY, Aug. 2010, p. 7592–7602 Vol. 84, No. 15
0022-538X/10/$12.00 doi:10.1128/JVI.00704-10

Congregation of Orthopoxvirus Virions in Cytoplasmic A-Type Inclusions Is Mediated by Interactions of a Bridging Protein (A26p) with a Matrix Protein (ATIp) and a Virion Membrane-Associated Protein (A27p)▽

Amanda R. Howard, Andrea S. Weisberg, and Bernard Moss*

Laboratory of Viral Diseases, National Institute of Allergy and Infectious Diseases, National Institutes of Health, Bethesda, Maryland 20892

Received 1 April 2010/Accepted 9 May 2010

Some orthopoxviruses, e.g., the cowpox, ectromelia, and raccoonpox viruses, form large, discrete cytoplasmic inclusions within which mature virions (MVs) are embedded by a process called occlusion. These inclusions, which may protect occluded MVs in the environment, are composed of aggregates of the A-type inclusion protein (ATIp), which is truncated in orthopoxviruses such as vaccinia virus (VACV) and variola virus that fail to form inclusions. In addition to an intact ATIp, occlusion requires the A26 protein (A26p). Although VACV contains a functional A26p, determined by complementation of a cowpox virus occlusion-defective mutant, its role in occlusion was unknown. We found that restoration of the full-length ATI gene was sufficient for VACV inclusion formation and the ensuing occlusion of MVs. A26p was present in inclusions even when virion assembly was inhibited, suggesting a direct interaction of A26p with ATIp. Analysis of a panel of ATIp mutants indicated that the C-terminal repeat region was required for inclusion formation and the N-terminal domain for interaction with A26p and occlusion. A26p is tethered to MVs via interaction with the A27 protein (A27p); A27p was not required for association of A26p with ATIp but was necessary for occlusion. In addition, the C-terminal domain of A26p, which mediates A26p-A27p interactions, was necessary but insufficient for occlusion. Taken together, the data suggest a model for occlusion in which A26p has a bridging role between ATIp and A27p, and A27p provides a link to the MV membrane.

The orthopoxviruses, which include the best-characterized and medically most significant members of the poxvirus family, produce two major types of infectious particles known as mature virions (MVs) and enveloped virions (5). MVs are assembled at cytoplasmic, juxtanuclear viral factories and consist of a core containing viral double-stranded genomic DNA, enzymes, and factors necessary for early gene transcription and structural proteins surrounded by a lipoprotein membrane. A population of MVs traffics along microtubules and acquires two additional membranes derived from *trans*-Golgi or endosomal cisternae to form wrapped virions. Wrapped virions traverse the cell along microtubules to the plasma membrane, where the outer viral membrane fuses with the plasma membrane to allow the exit of enveloped virions. However, the majority of MVs remain in the cytoplasm until cell lysis. The MVs of some orthopoxviruses, e.g., cowpox virus (CPXV), ectromelia virus, and raccoonpox virus, have an additional fate: they become embedded in dense, proteinaceous bodies called A-type inclusions (ATIs) that are distinguished from virus factories (6, 13, 14). Orthopoxviruses that do not form A-type inclusions include vaccinia virus (VACV), the prototype of the poxvirus family; variola virus, the causative agent of smallpox; and monkeypox virus, an emerging pathogen. Inclusions with embedded virions also form in cells infected with avipoxviruses and entomopoxviruses (3) and may protect virions from harsh environmental conditions during transmission between hosts.

ATIs form subsequent to viral DNA replication, and the matrix consists of a single known viral late protein, ATIp (18). ATIp is an abundant, high-molecular-mass (160 kDa in CPXV) hydrophobic protein that contains 14 repeats of about 30 amino acids each (8, 18). Orthopoxviruses that do not form inclusion bodies have mutated ATI genes. An ATIp homolog encoded by the A25L gene (VACVWR148) of the Western Reserve (WR) strain of VACV contains a deletion of two adenylate residues, resulting in synthesis of a C-terminally truncated, 94-kDa protein (1, 18). This A25 protein (A25p) contains the N-terminal half of ATIp, including the first four ATIp repeats and six amino acids of the fifth repeat. The embedding of MVs in inclusions requires a protein encoded by homologs of the A26L gene, which is mutated in some orthopoxvirus strains (15, 23). Although VACV does not form inclusion bodies, the VACV A26L gene (VACVWR149) is intact, and the VACV A26 protein (A26p) can complement the defective A26p homolog in the Brighton red (BR) strain of CPXV (CPXV-BR) (15). Whether VACV is missing other proteins needed for inclusion formation and occlusion was not known prior to the present study.

The mechanism by which A26p mediates occlusion had not been elucidated, although a role in retrograde transport of MVs was suggested (15). Recently, A26p was shown to be anchored to the MV membrane through disulfide bonding with

* Corresponding author. Mailing address: Laboratory of Viral Diseases, NIAID, NIH, 33 North Drive, MSC 3210, Bethesda, MD 20892-3210. Phone: (301) 496-9869. Fax: (301) 480-1535. E-mail: bmoss@nih.gov.

▽ Published ahead of print on 19 May 2010.

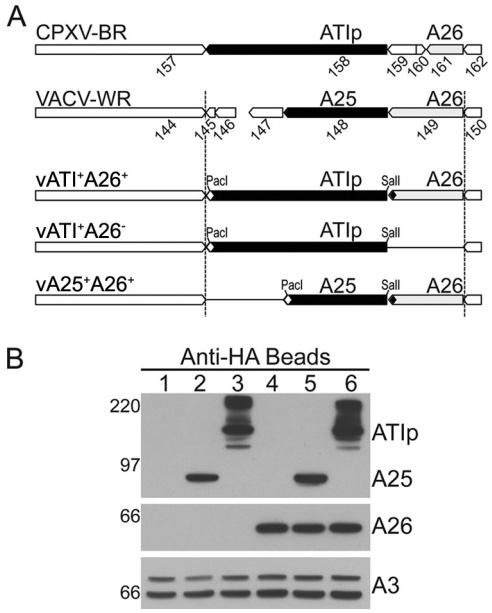

FIG. 1. Construction of recombinant VACV expressing ATIp. (A) Schematic drawings of the ATI and neighboring loci in CPXV-BR, VACV-WR, and recombinant VACV-WR. Recombinant viruses were made by replacing the truncated A25L gene (VACVWR148) with the full-length ATI gene (CPXVBR158) containing a C-terminal HA epitope tag or an A25L gene containing a C-terminal HA epitope tag (white diamond). The VACV A26L gene (VACVWR149) was either deleted or given a C-terminal V5-epitope tag (black diamond). The ATI and A25L genes are flanked by introduced SalI and PacI sites. Additional control viruses with deletions of A25L or A26L are not shown. (B) Western blot confirming expression of ATIp or A25p from recombinant viruses. Extracts of HeLa cells infected with $vA25^{-}A26^{-}$ (lane 1), $vA25^{+}A26^{-}$ (lane 2), $vATI^{+}A26^{-}$ (lane 3), $vA25^{-}A26^{+}$ (lane 4), $vA25^{+}A26^{+}$ (lane 5), or $vATI^{+}A26^{+}$ (lane 6) were resolved by SDS-PAGE under reducing conditions. ATIp and A25p were identified by using anti-HA antibodies and A26p was detected with anti-A26p antibodies. Precursor and processed forms of VACV late protein A3p were detected with antibody as a loading control. The sizes in kilodaltons and the electrophoretic positions of marker proteins are shown on the left.

the A27 protein (A27p) (4, 9), which is in turn tethered to the MV membrane through interactions with the A17 transmembrane protein (A17p) (19, 24). Our finding that A26p also interacts with A25p (9) suggested that it might similarly interact with the intact ATIp, thereby localizing MVs in inclusion bodies. To investigate the role of A26p in mediating occlusion, we constructed recombinant VACV expressing the CPXV-BR ATIp in place of the truncated VACV-WR A25p. Remarkably, this single alteration allowed VACV to produce typical inclusions containing MVs. Occlusion of MVs by recombinant VACV was dependent on both A26p and A27p, even though inclusions formed without either of these proteins. A26p localized with inclusions in the absence of A27p or MV production, a finding consistent with a direct interaction with ATIp. Separate domains of the ATIp were shown to be required for inclusion formation and association with A26p. Taken together, the data present a working model of occlusion in which A26p serves as a bridge between A27p on MVs and ATIp in inclusion bodies.

MATERIALS AND METHODS

Cells and viruses. African green monkey kidney BS-C-1 and human HeLa cell cultures were maintained in minimum essential medium with Earle's salts (Quality Biological, Gaithersburg, MD) and 10% fetal bovine serum (FBS). The medium was further supplemented with 2 mM L-glutamine, 100 U of penicillin/ml, and 100 μg of streptomycin/ml. Cells were infected with viruses in medium containing 2.5% FBS and the supplements listed above. Recombinant viruses were derived from the VACV-WR strain and the CPXV-BR strain and propagated as described previously (7).

Plasmid and recombinant virus construction. The following recombinant viruses were constructed by standard methods: (i) vA25HA.A26V5, which expresses an influenza virus hemagglutinin (HA) epitope-tagged VACV A25p and a V5-tagged VACV A26p; (ii) vATIHA.A26V5, which encodes an HA-tagged CPXV ATIp and a V5-tagged A26p; and (iii) vATIHA.ΔA26, which has A26L deleted and expresses an HA-tagged ATIp. In the first step, the VACV WR A25L gene was replaced by the enhanced green fluorescent protein (GFP) gene to generate vΔA25.GFP. Plasmids were then constructed to insert the cassettes of interest into the GFP locus of vΔA25.GFP. Briefly, the plasmids used to make vA25HA.A26V5 and vATIHA.A26V5 contained the left flanking region of the A25L open reading frame (ORF) with a PacI site introduced immediately downstream of the A25L stop codon. The right flanking region was amplified with DNA encoding a V5 tag introduced into to the C-terminal coding region of A26L and a SalI site immediately downstream of A26L and upstream of the A25L ORF. The two flanks were joined by overlap PCR using Accuprime *Pfx* (Invitrogen, Carlsbad, CA) and blunt-end ligated into pCR-BluntII-TOPO (Invitrogen) to generate the pFLANKS plasmid. pFLANKSΔA26 was constructed similarly to make vATIHA.ΔA26 except that the right flanking region was amplified from the A27L gene, which is immediately upstream of the A26L ORF. The VACV-WR A25L and CPXV-BR ATI genes and native promoters were amplified with forward and reverse primers introducing an upstream SalI site and DNA sequences coding for the HA tag with a downstream PacI site, respectively. The PCR products were subcloned into pCR-BluntII-TOPO, and the resulting plasmids were designated pA25HA and pATIHA. The ATIHA and A25HA inserts were excised from pA25HA and pATIHA using SalI and PacI for ligation with linearized pFLANKS and pFLANKSΔA26 to generate pFLANKS.A25HA, pFLANKS.ATIHA, and pFLANKSΔA26.ATIHA, respectively. vΔA25.GFP-infected cells were transfected with linearized pFLANKS.A25HA, pFLANKS.ATIHA, and pFLANKSΔA26.ATIHA using Lipofectamine 2000 (Invitrogen) according to the manufacturer's instructions. Control viruses with an A26L-A25L double deletion (vΔA25.ΔA26), an HA-fused A25L with a deleted A26L (vA25HA.ΔA26), and a deleted A25L with a V5-fused A26L (vΔA25.A26V5) were generated similarly to the methods described above. Recombinant viruses were clonally purified by consecutive rounds of white-plaque selection (7). The A4:YFP fusion was introduced as previously described (25).

The A27L deletion (vΔA27) virus containing the yellow fluorescent protein (YFP) fused to the N terminus of A4p was described previously (25). vΔA27 forms small plaques, and vΔA26.A4:YFP was generated from vΔA27 by inserting a cassette that deleted A26L but restored A27L at the A27L-A26L locus and selecting for large plaques.

The ATI deletion mutants were amplified from the pATIHA plasmid and cloned into the pTOPO vector. N-terminal deletion mutants were amplified using forward primers containing the CPXV-BR ATI promoter and an introduced start codon adjacent to at least the first 10 5′ nucleotides of the target sequence and a reverse primer to the HA tag. C-terminal mutants were amplified by using a forward primer complementary to the ATI promoter and a reverse primer overlapping the HA tag and stop codon with at least 10 nucleotides of the desired 3′ target.

pATIFLAG was generated by amplifying the ATI gene with a reverse primer coding for the FLAG epitope tag with the amino acid sequence DYKDDDDK. pA27HA, pA26V5, pA26ΔNV5, and pA26ΔCV5 were described previously (9).

Antibodies. Mouse monoclonal antibodies (MAbs) and rabbit polyclonal antibodies (PAbs) against the HA (YPYDVPDYA) and mouse MAbs against the V5 (GKPIPNPLLGLDST) epitope tags used for Western blotting were obtained from Covance (Princeton, NJ). Rabbit PAbs against A26p (9) and A3p (R. Doms and B. Moss, unpublished data) were also used for Western blotting. Immunofluorescence staining of the HA-tagged A25p, ATIp, and A27p was carried out using either rat MAbs (clone 3F10) from Roche Applied Sciences (Indianapolis, IN) or mouse MAbs or rabbit PAbs from Covance at 1:250 dilutions. Mouse MAbs and rabbit PAbs to V5, as well as mouse MAbs to FLAG were obtained from Sigma-Aldrich (St. Louis, MO). Mouse MAb to V5 from Abcam (Cambridge, MA) was also used. Alexa-conjugated anti-rat, anti-rabbit, and anti-mouse immunoglobulin G (IgG) antibodies were used at 1:250 (Invitrogen).

TABLE 1. Abbreviated nomenclature for recombinant viruses

Full name	Abbreviated name
vA25HA.A26V5.A4YFP	$vA25^{+}A26^{+}$
vATIHA.A26V5.A4YFP	$vATI^{+}A26^{+}$
vA25HA.ΔA26.A4YFP	$vA25^{+}A26^{-}$
vATIHA.ΔA26.A4YFP	$vATI^{+}A26^{-}$
vΔA25.A26V5.A4YFP	$vA25^{-}A26^{+}$
vΔA25.ΔA26.A4YFP	$vA25^{-}A26^{-}$
vΔA27.A4YFP	$vA27^{-}$

Immunoaffinity purification. As described previously (9), cells were solubilized in lysis buffer (150 mM NaCl, 50 mM Tris-HCl [pH 8.0], 1% NP-40) by rotating at 4°C for 30 min. The extracts were cleared and incubated with unconjugated agarose A-beads prior to incubation with mouse anti-V5 immunoaffinity beads (Sigma). Bound proteins were eluted by boiling beads in lithium dodecyl sulfate (LDS) loading buffer (Invitrogen). After the addition of reducing agent (Invitrogen), samples were resolved by sodium dodecyl sulfate-polyacrylamide gel electrophoresis (SDS-PAGE) using 4 to 12% NuPAGE Bis-Tris gels in NuPAGE morpholinepropanesulfonic acid running buffer (Invitrogen).

Western blotting. Whole-cell extracts for Western blotting were prepared by incubating virus-infected cells in 10 mM Tris-HCl (pH 7.4), 10 mM $CaCl_2$, and 10 mM NaCl with 8 μg of micrococcal nuclease/ml and 0.5% NP-40 for 30 min on ice, followed by brief sonication (22). LDS and reducing agent were added, and the samples were boiled prior to resolution by SDS-PAGE as described above. Proteins were transferred electrophoretically to a nitrocellulose membrane and detected using antibodies as described above and anti-rabbit or anti-mouse IgG conjugated to horseradish peroxidase (Pierce, Rockford, IL), which was developed by using SuperSignal chemiluminescent substrates (Pierce).

Infection and transfection. Dishes with 24 wells containing coverslips seeded with ~2.5×10^5 HeLa cells for confocal microscopy were infected at a multiplicity of infection of 0.1 PFU per cell in Opti-MEM (Invitrogen). After 1 h, the cells were washed and transfected with 200 ng of plasmid using Lipofectamine 2000 (Invitrogen) according to the manufacturer's recommendations (9).

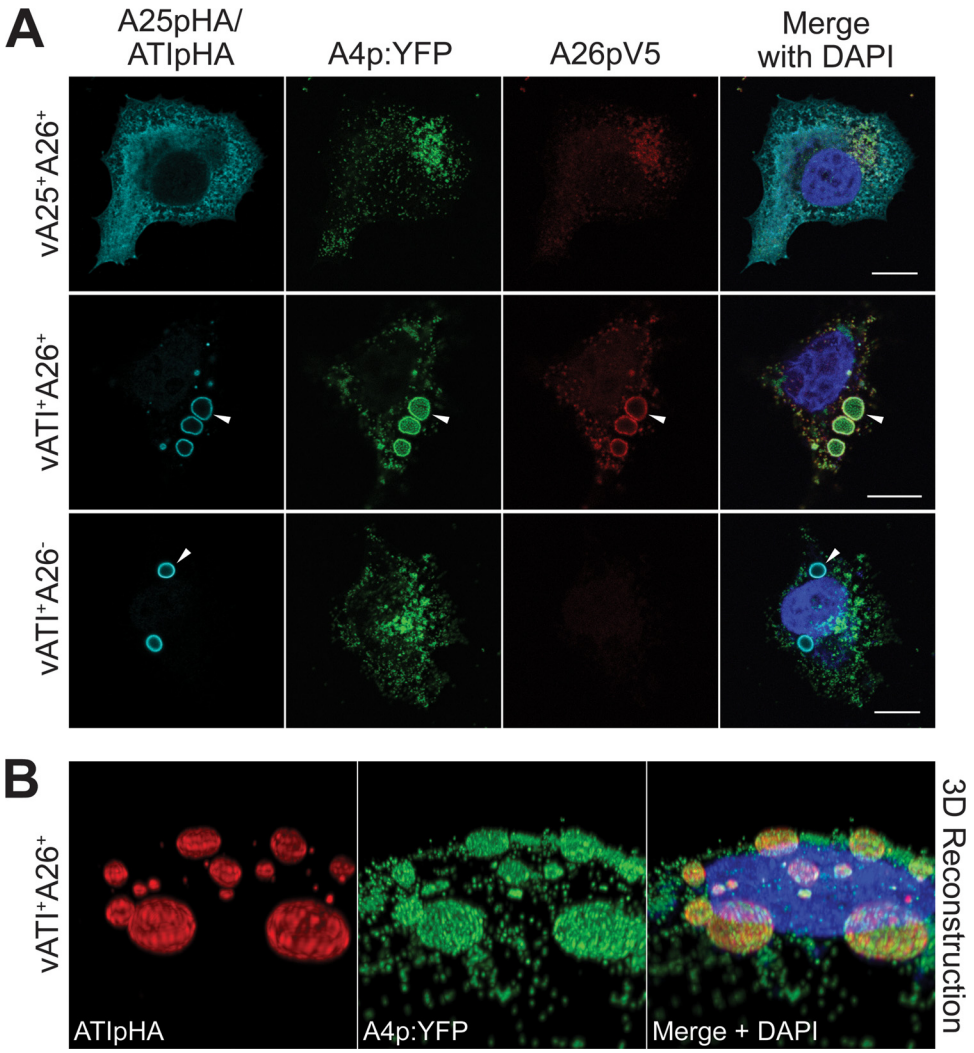

FIG. 2. Recombinant VACV inclusion body formation and occlusion. (A) Confocal microscopic images of HeLa cells infected with $vA25^{+}A26^{+}$ (top row), $vATI^{+}A26^{+}$ (middle row), and $vATI^{+}A26^{-}$ (bottom row) were fixed, permeabilized, and stained at 18 h after infection. DAPI used to stain DNA in the nucleus and viral factories (blue) is shown in the merge. Rabbit anti-HA antibodies, followed by Alexa 647-conjugated anti-rabbit IgG, were used to stain A25p and ATIp (cyan). MV particles were visualized using YFP fluorescence (green). Mouse anti-V5 antibodies, followed by Alexa 594-conjugated anti-mouse IgG, were used to stain A26p (red). Inclusion bodies are denoted by arrowheads. Scale bars, 10 μm. (B) Three-dimensional reconstruction of cell infected with $vATI^{+}A26^{+}$ at 18 h postinfection and stained as described above. ATIpHA (red) staining shows inclusion bodies are quasispherical and A4p:YFP fluorescence (green) reveals MV filling inclusions.

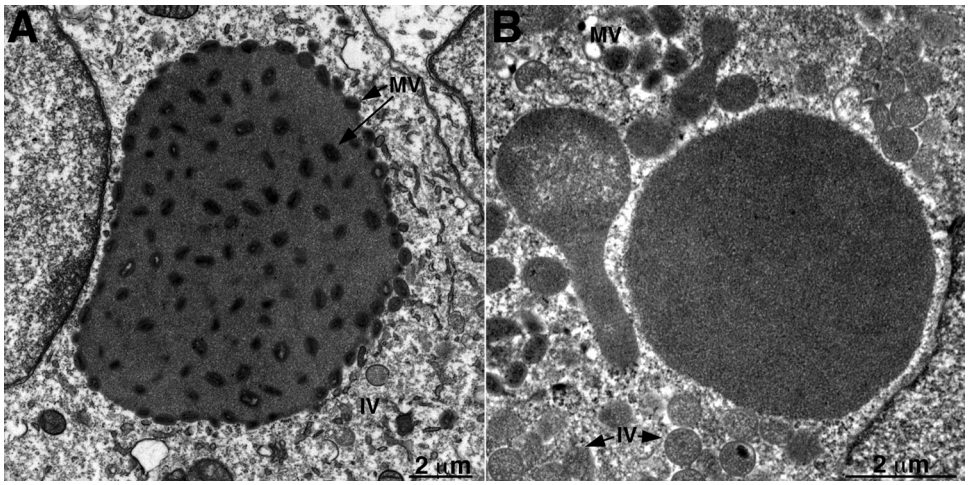

FIG. 3. Transmission electron microscopy of inclusion bodies. BS-C-1 cells infected with 10 PFU of vATI$^+$A26$^+$ (A) or vATI$^+$A26$^-$ (B) per cell were fixed at 24 h after infection. Electron microscopic images of thin sections are shown. Representative MVs and immature virions (IV) are labeled. Scale bars, 2 μm.

Confocal microscopy. HeLa cells were washed three times at room temperature in Dulbecco phosphate-buffered saline (PBS) without Ca^{2+} and Mg^{2+} prior to fixation for 10 min in 4% paraformaldehyde in PBS. The cells were washed four times and permeabilized with 0.2% Triton X-100 for 7 min. Four 5-min washes in PBS were used to ensure the removal of Triton X-100. Prior to staining, the cells were blocked in 10% FBS-PBS for 1 h. Primary staining was carried out at room temperature for 1 h in 10% FBS-PBS. Four 5-min washes in PBS were used to remove any unbound antibody, and secondary staining was carried out in 10% FBS-PBS for 45 min. Cells were subjected to four 5-min PBS washes, and coverslips were mounted onto slides using ProLong Gold with or without DAPI (4′,6′-diamidino-2-phenylindole) mounting medium (Invitrogen). A Leica SP2 inverted four-channel microscope was used for imaging. Select images were deconvolved using Huygens Essential version 3.5.0 (64 bit; Scientific Volume Imaging, Hilversum, Netherlands), and the brightness and contrast were adjusted by using either Imaris Bitplane Scientific Software version 6.4.2 (St. Paul, MN) or Adobe Photoshop CS3 (Adobe Systems, San Jose, CA).

Electron microscopy. BS-C-1 cells in 60-mm-diameter dishes were infected with recombinant viruses at a multiplicity of infection of 10 PFU/cell. Cells were fixed with 2% glutaraldehyde at 22 h postinfection and embedded in EmBed-182 resin (Electron Microscopy Sciences, Hatfield, PA). Samples were viewed with a FEI Tecnai Spirit transmission electron microscope (Hillsboro, OR).

RESULTS

Restoration of full-length ATIp allows inclusion body formation in cells infected with recombinant VACV. We were interested in determining whether replacement of the disrupted ATI gene of VACV with the full-length CPXV homolog would be sufficient to support inclusion body formation and occlusion for two main reasons: a negative result would suggest the need for additional CPXV genes, which we would then try to identify; a positive result would allow us to study occlusion in the VACV background, which is better characterized than that of CPXV. The region of CPXV-BR encoding the full-length 1,284-amino-acid ATIp (ORF 158) and the disrupted A26p homolog (ORFs 159, 160, and 161) is shown in Fig. 1A. In contrast, four smaller ORFs (145, 146, 147, and 148) comprise the disrupted ATIp homolog of VACV-WR, whereas ORF 149 encoding A26p is intact (Fig. 1A). VACV ORF 148, encoding the expressed 725-amino acid A25p, has a late promoter, whereas ORFs 145, 146, and 147 are probably not expressed since they lack recognizable promoters. To avoid potential complications due to recombination during the reconstruction of the VACV genome, ORFs 145 to 148 were deleted from the VACV genome prior to insertion of the complete CPXV-BR ATI gene with a C-terminal HA epitope tag and the native late ATI promoter. The VACV ORF encoding A26p was replaced with a V5-tagged version or deleted (Fig. 1A.). Another recombinant virus was constructed encoding an HA-tagged VACV A25p and a V5-tagged VACV A26p to be used as a control that does not form inclusion bodies. In each case, the YFP ORF was fused to the ORF encoding the VACV core protein A4p (A4YFP) to visualize MV by confocal microscopy. The A4YFP fusion has been used previously to monitor virion localization and movement (25). The recombinant viruses formed normal looking plaques (data not shown), indicating that the genome alterations had little or no effect on replication. Because use of the full descriptive names of the recombinant viruses is cumbersome, we will generally omit reference to the epitope tags and YFP fusion and simply refer to recombinant viruses with intact ATIHA as ATI$^+$, A25HA as A25$^+$, and A26V5 as A26$^+$ as indicated in Table 1. Viruses with a deletion of A25 or A26 are referred to as A25$^-$ or A26$^-$ (Table 1).

Whole-cell lysates from cells infected with vATI$^+$A26$^+$ and vA25$^+$A26$^+$ or with control viruses missing one or two genes (vATI$^+$A26$^-$, vA25$^+$A26$^-$, vA25$^-$A26$^+$, and vA25$^-$A26$^-$) were analyzed by Western blotting to determine whether the CPXV-BR ATIp was expressed in the VACV background. Proteins were resolved by SDS-PAGE under reducing conditions, and anti-HA antibodies revealed bands migrating to positions corresponding to the expected masses of ca. 94 and 160 kDa for A25p and ATIp, respectively (Fig. 1B). Slower-migrating bands, which presumably represent incompletely dissociated oligomeric forms of ATIp, were also detected in samples from vATI$^+$A26$^+$- and vATI$^+$A26$^-$-infected cells. In contrast, SDS-resistant oligomeric forms of A25p were not detected. Bands representing lower-molecular-mass processed species of both A25p and A26p were also detected by Western blotting (shown later). A26p was resolved as a 60-kDa protein

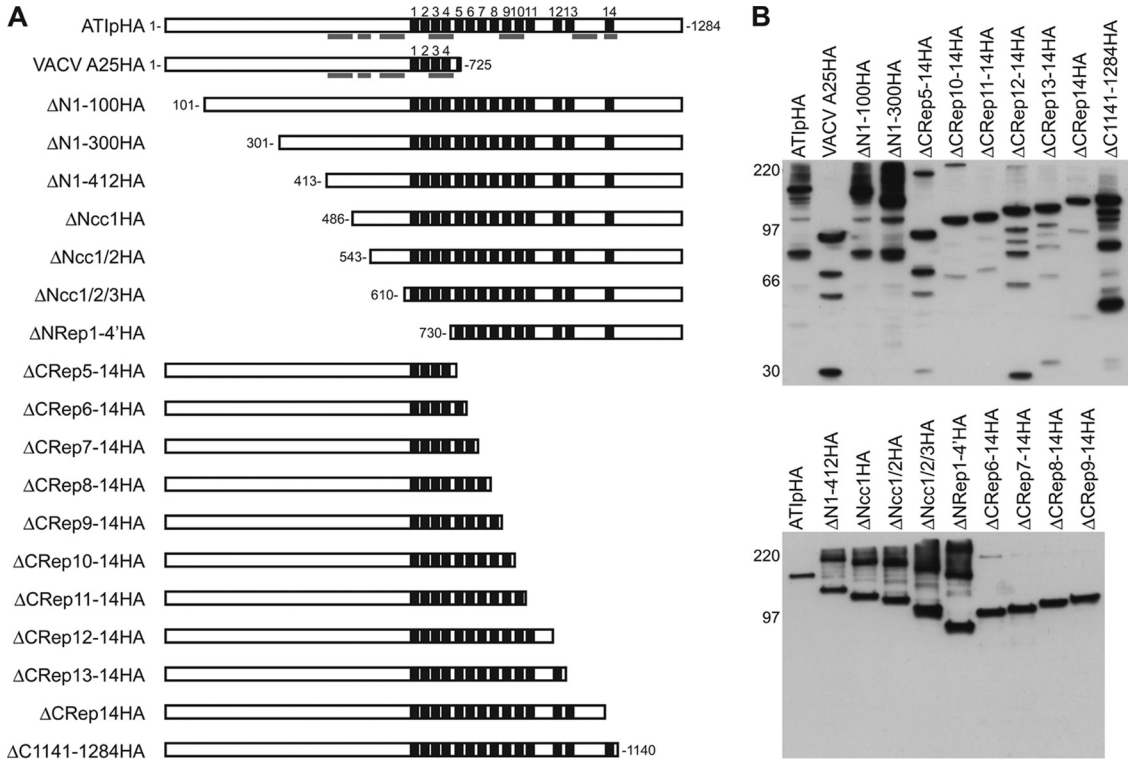

FIG. 4. Construction and expression of truncated ATIps. (A) Schematic of ATIp and N- and C-terminal truncated versions with C-terminal HA tag. The 14 ATIp repeats (black boxes) are numbered. Gray bars represent predicted coiled-coil domains. "ΔN" followed by numbers indicates the amino acids deleted from the N terminus; "ΔNcc" followed by numbers indicates deletion of coiled-coil domains from the N terminus; "ΔNRep" followed by a numbers indicates the deletion of repeat sequences from the N terminus; "ΔCRep" followed by numbers indicates the deletion of repeat sequences from the C terminus; "ΔC" followed by numbers indicates amino acids deleted from the C terminus. (B) Detection of HA-tagged ATIp and truncated forms by Western blotting. Proteins from BS-C-1 cells infected with $vA25^{-}A26^{+}$ and transfected with plasmids expressing ATIp and truncation mutants were resolved by SDS-PAGE under reducing conditions, transferred to a nitrocellulose membrane, and detected by chemiluminescence after probing with antibody to the HA epitope tag. The positions of marker proteins in kilodaltons are shown on the left.

detected by Western blotting with anti-A26p antibodies in lysates from cells infected with $vA25^{-}A26^{+}$, $vA25^{+}A26^{+}$, and $vATI^{+}A26^{+}$ but not with $vA25^{-}A26^{-}$, $vA25^{+}A26^{-}$, and $vATI^{+}A26^{-}$ (Fig. 1B). Antibody to the A3p VACV core protein was used as a loading control.

After determining that ATIp was expressed in cells infected with $vATI^{+}A26^{+}$ and $vATI^{+}A26^{-}$, we investigated the formation of inclusion bodies by confocal microscopy. HeLa cells were infected with $vA25^{+}A26^{+}$, $vATI^{+}A26^{+}$, or $vATI^{+}A26^{-}$ and fixed 18 h later. The cell nucleus and DNA factories, which were moderately dispersed at this late time, were visualized by DAPI staining. Anti-HA staining was used to detect A25p or ATIp, and anti-V5 staining was used for A26p localization. In cells infected with $vA25^{+}A26^{+}$, the A4:YFP core protein partially colocalized with virus factories and with punctate structures, presumably representing virus particles distributed throughout the cytoplasm (Fig. 2A, top row). A26p colocalized with A4p:YFP, whereas the abundant A25p was diffusely distributed (Fig. 2A, top row). Western blotting and immunoprecipitation experiments carried out using purified $vA25^{+}A26^{+}$ virions showed that the HA tag did not disrupt either the virion association of A25 or the A26-A25 interaction (data not shown).

Optical sections of cells infected with $vATI^{+}A26^{+}$ and stained with antibodies that recognized the HA tag on ATIp revealed distinct ringlike structures (Fig. 2A, middle row) in contrast to the diffuse staining of A25p (Fig. 2A, top row). Similar peripheral staining patterns of inclusion bodies by anti-ATIp antibodies were seen in previous studies in which the authors suggested that inclusion bodies are impermeable to the antibody conjugate (18). MV particles, detected by the YFP fluorescence, were associated with ATI as early as 8 h (not shown) and encrusted and filled the inclusions by 18 h (Fig. 2A, middle row). Anti-V5 staining showed that A26p was associated with the inclusions and nonoccluded MVs (Fig. 2A). The anti-V5 staining decorated the outside of the ATI bodies and was virtually undetectable in their interior, presumably due to antibody inaccessibility. Three-dimensional reconstructions (Imaris Bitplane Scientific Software, St. Paul, MN) of optical sections of $vATI^{+}A26^{+}$-infected cells showed the peripherally stained inclusions as quasispherical bodies studded or packed with A4-YFP-fluorescing MV particles (Fig. 2B).

In cells infected with $vATI^{+}A26^{-}$, inclusion bodies formed but MV particles did not associate with them (Fig. 2A, bottom row), confirming the requirement for A26p as observed previously for CPXV mutants (10–12, 15). These experiments indicated that expression of the full-length ATIp conferred upon VACV the ability to form inclusions and to occlude MVs.

Thus, VACV-WR encodes all viral proteins needed for occlusion except for the full-length ATIp.

Fine structure of VACV inclusion bodies. Transmission electron microscopy was used to visualize inclusion bodies and associated MVs at higher magnification. Sections were prepared from BS-C-1 cells infected with either vATI$^+$A26$^+$ or vATI$^+$A26$^-$ at 22 h postinfection. In cells infected with vATI$^+$A26$^+$, characteristic large, electron-dense granular inclusion bodies were seen, and MVs were embedded throughout the proteinaceous matrices of most (Fig. 3A). Other forms of VACV, including immature and wrapped virions, were not closely associated with inclusion bodies. Inclusion bodies also formed in cells infected with vATI$^+$A26$^-$, but MVs were not occluded (Fig. 3B).

Construction and expression of ATIp truncation mutants. To distinguish the domains of ATIp necessary for formation of inclusion bodies and for occlusion of MVs, a panel of plasmids expressing N-terminal or C-terminal truncated ATIps was constructed. Each mutant ATIp had a C-terminal HA epitope tag to allow detection. Mutants ΔN1-100, ΔN1-300, and ΔN1-412 have N-terminal deletions of 100, 300, and 412 amino acids, respectively (Fig. 4A). Mutants ΔNcc1, ΔNcc1/2, and ΔNcc1/2/3 have more extensive N-terminal deletions extending through the first, second, and third coil-coil domains, respectively (Fig. 4A). The entire N-terminal half of the protein including repeats 1 to 4 was deleted in the mutant ΔNRep1-4′. A set of C-terminal truncations was made by incrementally deleting repeats up to the amino acid sequences included in A25p (Fig. 4A).

To examine expression of the mutant proteins, BS-C-1 cells infected with vA25$^-$A26$^+$ were transfected with plasmids encoding the mutant ATIps regulated by the natural ATIp promoter. Proteins in whole-cell lysates were resolved by SDS-PAGE under reducing conditions and transferred to nitrocellulose membranes for Western blotting with anti-HA antibodies. Prominent bands migrated to positions corresponding to the reported 160 kDa for ATIp and 94 kDa for VACV A25p, as well as the predicted masses of the mutant proteins (Fig. 4B). Multiple bands were detected for ATIp, A25p, and ATIp mutants, presumably representing larger oligomeric and smaller processed forms of the proteins (Fig. 4B).

Effects of N- and C-terminal truncations of ATIp on inclusion formation. The inability of VACV expressing the C-terminally truncated A25p to form inclusions and the repair of this defect by substituting the CPXV ATIp suggested the importance of the added repeats. To map the domains of ATIp required for inclusion formation and occlusion, HeLa cells were infected with vA25$^-$A26$^+$ and transfected with the panel of plasmids shown in Fig. 4A. Cells were fixed at 16 h after transfection, immunostained, and analyzed by confocal microscopy. The results of these experiments are summarized in Table 2, and confocal microscopy images of selected mutants are shown in Fig. 5. In this section, we discuss the effects of the mutations on inclusion body formation; the effects on A26p and MV localization are noted in the following section. Typical inclusion bodies with ring-like antibody staining formed in all cells transfected with pATIpHA (Fig. 5). N-terminal truncations of ATIp up to the repeats did not abrogate inclusion formation, although inclusions had an altered architecture appearing as lamellar structures (Fig. 5, pΔN1-100HA, pΔN1-300HA, and pΔNcc1/2/3HA) that sometimes occupied the bulk of the cytoplasm (data not shown). However, deletion of the first four repeats plus the first 6 amino acids of repeat 5 (pΔNRep1-4′) disrupted inclusion formation, even though the protein still contained nine intact repeats (Fig. 5).

TABLE 2. Summary of the effects of deletion mutations on inclusion formation, A26p localization, and MV occlusion

Mutant	Effect[a] on:		
	Inclusion formation[b]	A26 localization	MV occlusion
ΔN1-100HA	+	+	–
ΔN1-300HA	+	–	–
ΔN1-412HA	+	–	–
ΔNcc1HA	+	–	–
ΔNcc1/2HA	+	–	–
ΔNcc1/2/3HA	+	–	–
ΔNRep1-4′	–	–*	NA
ΔCRep5-14HA	–	+*	NA
ΔCRep6-14HA	–	+*	NA
ΔCRep7-14HA	+/–	+*	NA
ΔCRep8-14HA	+/–	+	+
ΔCRep9-14HA	+	+	+
ΔCRep10-14HA	+	+	+
ΔCRep11-14HA	+	+	+
ΔCRep12-14HA	+	+	+
ΔCRep13-14HA	+	+	+
ΔCRep14HA	+	+	+
ΔC1141-1284HA	+	+	+

[a] A26 and MV localization were scored as "+" or "–". NA, not applicable since there were no inclusions. *, Proteins that did not form inclusion bodies or formed few inclusion bodies were tested for interaction with A26p by immunoprecipitation.

[b] Approximately 100 cells infected with vA25$^-$A26$^+$ and transfected with plasmids expressing mutant ATIps from at least two separate experiments were analyzed. Wild-type and mutant ATIp aggregates of >0.4 μm were scored as inclusion bodies. Inclusion formation is indicated as "+", "+/–", or "–" based on the number of cells expressing the mutant protein that contained inclusion bodies: +, >50% cells contain inclusion bodies; +/–, <50% but >20%; –, <20%.

The C-terminal truncation mutants were analyzed similarly. Truncation through repeats 12 to 14 did not alter architecture of inclusion bodies (Fig. 5). Inclusions formed by ATIp truncation through repeats 10 and 11 also resembled wild-type inclusions in shape, but staining revealed a greater amount of unincorporated protein in the cytoplasm (data not shown). As additional repeats were deleted from the C-terminal end of ATIp, the inclusions became smaller and less discrete and were detected in a lower percentage of cells, e.g., 60, 32, 22, and 8% of cells transfected with pΔCRep9-14, pΔCRep8-14, pΔCRep7-14, and pΔCRep6-14, respectively (Fig. 5). The pΔCRep8-14HA and pΔCRep7-14HA proteins formed small, irregular inclusion bodies (Fig. 5 and data not shown). The pΔCRep6-14HA localization in the cell resembled that of A25HA (Fig. 5). These results demonstrated a role for the N-terminal sequence of ATIp, as well as repeats 1 to 4 (and possibly the first 6 amino acids of repeat 5), plus an additional three or more repeats of ATIp for inclusion formation.

Effects of N- and C-terminal truncations of ATIp on A26p association and occlusion. In the experiments described above, A26p and MV localization were also examined. The first 100 amino acids of ATIp were dispensable for ATIp-A26p colocalization, even though the inclusions had an atypical appearance (Fig. 5, Table 2). However, the truncated ATI proteins

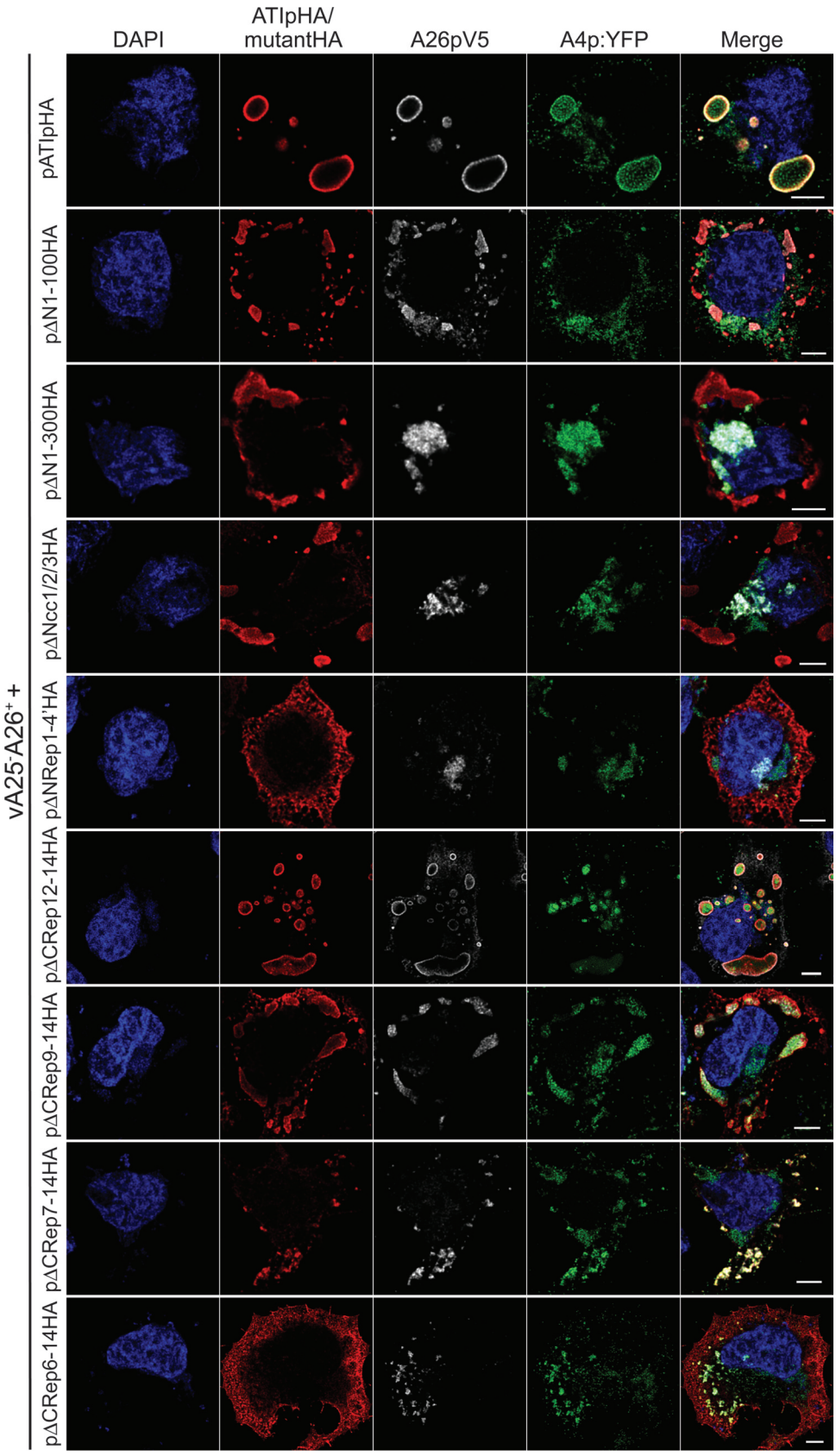

FIG. 5. Effects of ATIp mutations on inclusion formation, A26p localization, and MV occlusion. BS-C-1 cells were infected and transfected as described in the legend to Fig. 4. Representative confocal microscopic sections of selected N- and C-terminal deletion mutant ATIps are shown. Rabbit anti-HA antibodies, followed by Alexa-594 conjugated anti-rabbit IgG, were used to identify inclusion bodies. Mouse anti-V5 antibodies, followed by Alexa-647 conjugated anti-rabbit IgG, were used to visualize A26pV5. MVs were detected by YFP fluorescence due to A4 fusion protein. Blue, DAPI; red, Alexa 594; white, Alexa 647; green, A4:YFP.

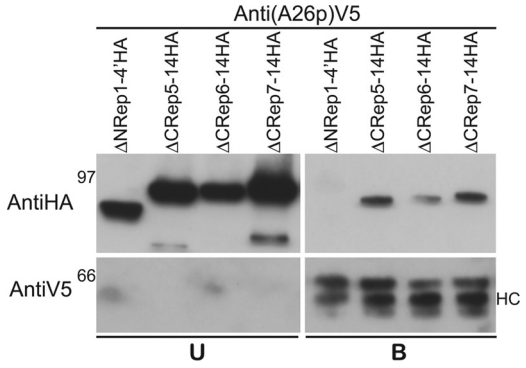

FIG. 6. Coimmunoprecipitation of truncated ATIps with A26pV5. Cells were infected with vA25$^-$A26$^-$ and cotransfected with pA26V5 and plasmids expressing N-terminal (ΔNRep1-4′HA) or C-terminal (ΔCRep5-14HA, ΔCRep6-14HA, and ΔCRep7-14) ATIp truncation mutants that do not form inclusion bodies. Cells lysates were cleared and incubated with mouse anti-V5-conjugated affinity agarose beads. Unbound (U) and bound fractions eluted from beads with LDS sample buffer (B) were resolved by SDS-PAGE, transferred to nitrocellulose membrane, and probed with mouse anti-HA antibody to detect ATIp (upper panels) and mouse anti-V5 antibody (lower panels) to detect A26p. Positions of 97- and 66-kDa marker proteins are indicated on the left. HC, IgG heavy chain.

pΔN1-300HA through pΔNRep1-4′HA did not colocalize with A26p, demonstrating that ATIp-A26p interactions are mediated through the N-terminal half of the ATIp protein (Fig. 5, Table 2). Furthermore, mutations that disrupted the ability of ATIp to interact with A26p disrupted MV occlusion as determined by A4p:YFP fluorescence (Fig. 5, Table 2). Although A26p localized to inclusion bodies formed by pΔN1-100HA, MVs were not embedded in these bodies (Fig. 5), perhaps due to the aberrant structure of the ATIs. A26p and MV localized to the C-terminal mutants of ATIp that retained the ability to form inclusion bodies (Fig. 5, Table 2).

It was impossible to use immunoprecipitation to study interactions of A26p with ATIps that formed inclusions because of solubility problems even in the presence of nondenaturing detergents. However, we could use immunoprecipitation to determine whether soluble ATIp mutants that did not form inclusion bodies were able to interact with A26p. BS-C-1 cells were infected with vA25$^-$A26$^-$ and cotransfected with pA26V5 and plasmids expressing the N-terminal ATI truncations pΔNRep1-4′HA or the C-terminal ATI truncations pΔCRep5-14HA, pΔCRep6-14HA, or pΔCRep7-14, respectively. Detergent-disrupted cell lysates were incubated with mouse anti-V5 conjugated agarose beads to bind A26p and associated proteins, and unbound and bound fractions were resolved by SDS-PAGE and analyzed by Western blotting. The C-terminal truncated proteins pΔCRep5-14HA, pΔCRep6-14HA, and pΔCRep7-14 were associated with A26p and present in the bound fractions (Fig. 6). However, the N-terminal truncated protein, pΔNRep1-4′HA, was absent from the bound fraction and present only in the unbound fraction, confirming that A26p-ATIp interactions are mediated by the N terminus of the ATIp (Fig. 6).

A27p is required for congregation of MVs in inclusion bodies but not for localization of A26p. VACV A27p anchors A26p to the MV particle through disulfide interactions with the C terminus of A26p (4, 9). The association of the VACV A25p with the A26p-A27p complex suggested that A26p bridges MV with inclusion bodies through interactions with A27p on the MV membrane and ATIp, respectively. To test whether A27p is required for occlusion, we infected cells with the A27 deletion mutant vA27$^-$ (Table 1), which lacks an intact ATI gene and contains A4:YFP, and transfected plasmids expressing FLAG-tagged ATIp and V5-tagged A26p with or without plasmids expressing HA-tagged A27p. ATIpFLAG formed inclusion bodies when transfected into cells infected with vA27$^-$. However, the YFP fluorescent MV particles did not localize in inclusion bodies in the absence of A27p (Fig. 7A). Occlusion was not rescued in cells infected with vA27$^-$ and transfected with a plasmid overexpressing A26V5p in addition to ATIpFLAG, although A26V5p did localize to inclusion bodies under these conditions (Fig. 7A). The ability of MV to embed within inclusion bodies in cells infected with vA27$^-$ was rescued by A27p expressed from plasmids cotransfected with pATIpFLAG and pA26V5 (Fig. 7A). The data indicated a role for A27 in occlusion, likely by tethering A26p to the MV membrane.

The experiment described above also demonstrated that A26p could traffic to inclusions in the absence of MVs. To confirm this result, cells were infected with vATI$^+$A26$^+$ for 9 h in the presence of the drug rifampin, which interrupts assembly at a stage prior to crescent membrane formation (16, 17). A26p localized to inclusion bodies in the absence of virion assembly, demonstrating that A26p traffics to inclusions in the absence of MV association (Fig. 7B).

The MV anchoring domain of A26p is required but not sufficient for occlusion. We previously determined that the C-terminal 100 amino acids of A26p are required for A26p-A27p disulfide interactions and anchoring to the MV membrane (9). Subsequently, it was shown that two conserved cysteines in the A26p C terminus specifically mediate A26-A27 interactions (4). We used two previously characterized truncated A26p mutants to test whether anchoring to the MV membrane is required for directing particle occlusion. The plasmid pA26ΔNV5 expresses the C-terminal 270 to 500 amino acids of A26p and is sufficient for interaction with A27p, whereas pA26ΔCV5, which codes for amino acids 1 to 409 of A26p, is not. Cells were infected with the A25p and A26p double deletion virus expressing A4:YFP (vA25$^-$A26$^-$) and cotransfected with pATIHA and pA26V5, pA26ΔCV5, or pA26ΔNV5. Cells infected with vA25$^-$A26$^-$ and cotransfected with pATIHA and pA26V5 contained inclusion bodies to which A26pV5 and virions localized (Fig. 8). A26ΔCpV5 localized to inclusion bodies but was not associated with virions, demonstrating that A26-MV anchoring is required for the occlusion of MV within inclusion bodies. In contrast, A26ΔNpV5 was strongly coincident with virions, but neither A26ΔNpV5 nor MV localized to inclusion bodies (Fig. 8), suggesting that the N terminus, although dispensable for A26-A27 interactions, was required for association with inclusion bodies.

DISCUSSION

The embedding of virions in dense proteinaceous masses is a strategy used by some DNA viruses to enhance their stability upon release into the environment. This capability is preserved

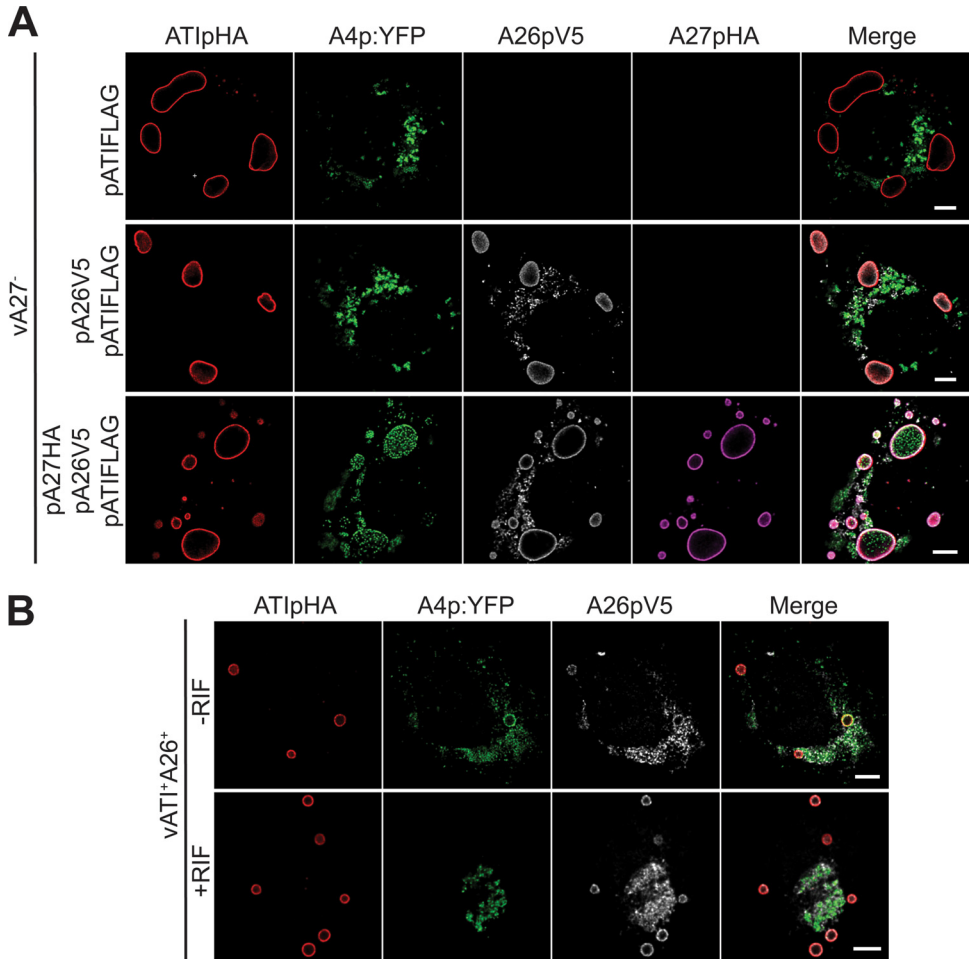

FIG. 7. Requirement for A27p for virion occlusion. (A) HeLa cells were infected with an A27 deletion VACV expressing YFP fused to the core protein A4 and lacking an intact ATI gene (vA27^{-}, Table 1). Cells were transfected with pATIFLAG alone (top row); pATIFLAG and pA26V5 (middle row); or pATIFLAG, pA26V5, and pA27HA (bottom row). At 18 h after transfection, the cells were fixed and permeabilized. ATIp (red) was detected with mouse anti-FLAG antibodies, followed by Alexa 405 conjugated anti-mouse IgG. The A27pHA (magenta) and A26pV5 (white) proteins were visualized using rat anti-HA and rabbit anti-V5 antibodies, followed by Alexa 647- and Alexa 594-conjugated anti-rat and anti-rabbit IgG, respectively. MVs were detected by YFP fluorescence (green). (B) Cells were infected with vATI^{+}A26^{+} for 9 h in the presence of the drug rifampin, which blocks virion assembly. ATIpHA (red) and A26pV5 (white) were visualized using rat anti-HA and rabbit anti-V5 antibodies, followed by Alexa 405-conjugated anti-rabbit IgG and Alexa 594-conjugated anti-rabbit IgG, respectively. MVs were detected by A4p:YFP fluorescence (green). Scale bars, 5 μm.

by some orthopoxviruses but lost by others. Previous studies had shown that CPXV inclusions consist predominantly or exclusively of the 160-kDa ATIp (18). However, some CPXV mutants that have an intact ATIp and can form inclusions fail to occlude virions. This defect is due to a mutation of the CPXV homolog of the VACV A26p (15). Nevertheless, how A26p mediates occlusion was not understood. The discovery that the A26p interacts with both MV membrane-bound A27p-A17p complex and the truncated VACV ATIp homolog A25p suggested a bridging role for A26p in occlusion (9).

We explored the validity of the above occlusion model using recombinant VACV rather than CPXV for two main reasons. First, VACV is better characterized than CPXV, and more mutants and reagents are available. Second, we wanted to determine whether restoration of the full-length ATIp would be sufficient for both occlusion and inclusion formation in VACV-infected cells. If restoration of the ATIp failed to allow occlusion, then it would suggest a role for additional viral proteins. Remarkably, exchanging the truncated A25p of VACV-WR with the full-length ATIp of CPXV-BR was sufficient for inclusion formation, as well as the occlusion of MVs. Indeed, the VACV ATI was indistinguishable from the CPXV ATI by electron microscopy.

A panel of plasmids expressing ATIp mutants was constructed to investigate the domains needed for inclusion formation, interaction with A26p, and occlusion of MVs. Mutational analysis of ATIp revealed that domains essential for inclusion formation are contained in the C-terminal ATI repeat region of the protein. Inclusion formation required ATI repeats 1 to 4 and possibly the first 6 amino acids of repeat 5, which are present in A25p, plus at least three additional repeats. In general, a higher percentage of cells formed inclusions with more ATI repeats. N-terminal deletions of ATIp did not prevent inclusion body formation, but their appearance

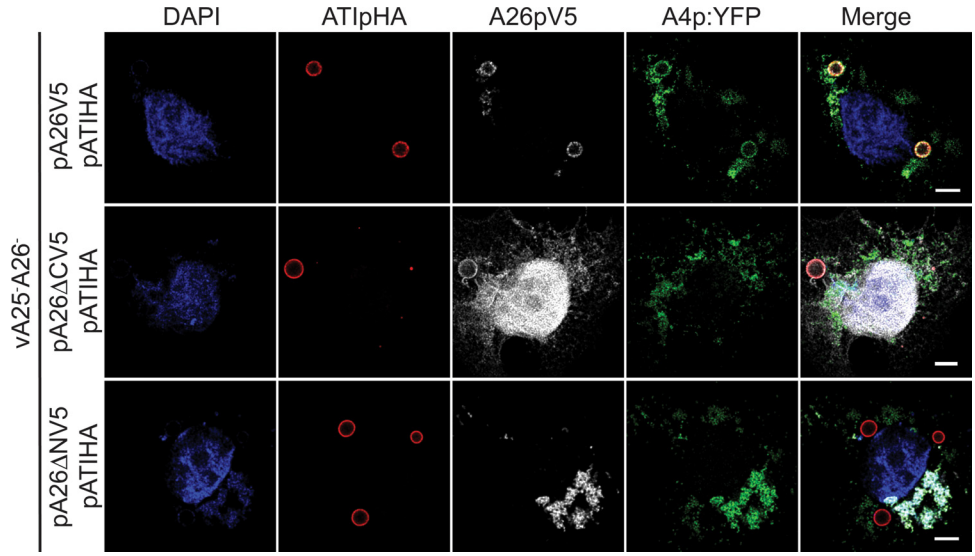

FIG. 8. Requirements of A26p N- and C-terminal domains for virion occlusion. HeLa cells were infected with vA25^{-}A26^{-} and transfected with pATIpHA and cotransfected with pA26V5, pA26ΔCV5, or pA26ΔNV5. At 18 h after transfection, ATIpHA (red) was stained with rat anti-HA antibodies, followed by Alexa 405-conjugated anti-mouse IgG. A26pV5 and mutants (white) were visualized by using rabbit anti-V5, followed by Alexa 594-conjugated anti-rabbit IgG. MV localization was monitored using A4p:YFP fluorescence (green). Blue, DAPI. Note that A26ΔCV5 also localized to nucleus. Scale bars, 5 μm.

was altered and lamellar structures were observed. We found that the N-terminal region of ATIp was needed for interaction with A26p. Even though deletion of the entire repeat region of ATIp abrogated inclusion formation, the truncated protein was still able to interact with A26p, as determined by both microscopic localization studies and immunoprecipitation experiments. Furthermore, mutations in ATIp that prevented its interaction with A26p also blocked occlusion, indicating an essential role for A26-ATIp interactions. Our data suggest that multiple ATI repeats are needed for aggregation of ATIp to form inclusions and that the N-terminal region of ATIp is needed for interaction with A26p.

We further investigated the need to anchor A26p to the MV particle for occlusion. Initial characterization of occlusion by Shida et al. (20) suggested that the p4c protein, subsequently shown to be A26p (15), functions to mediate occlusion as a virion component. Since we had shown that A26p is anchored to the MV by the A27p-A17p complex, we predicted that A27p would be required for occlusion. Indeed, A26p was not sufficient to direct occlusion in the absence of A27p. Moreover, an A26p C-terminal deletion mutant that does not interact with A27p did not mediate occlusion. Nevertheless, the mutant A26p still localized to inclusion bodies, even though it was not associated with virus particles, suggesting that the N terminus of A26p interacts directly with ATIp. On the other hand, an N-terminal deletion mutant of A26p that does not disrupt A26p-A27p interactions localized to virions in the cytoplasm of infected cells but was unable to mediate occlusion or localize to inclusion bodies.

Our studies indicated that A26p has a bridging function enabling the association of MVs containing membrane-associated A27p with the ATIp in inclusions. This model can explain why immature virions are not occluded since A27p is incorporated into virions at a later stage (21), presumably after the D13 scaffold has been removed (2). The large size of MVs and the distance between the sites of their assembly in factories and inclusion bodies make it unlikely that occlusion is a totally passive phenomenon. McKelvey et al. (15) suggested that A26p might be involved in retrograde movement of MVs in the cytoplasm. We are currently trying to determine whether microtubules are involved in the occlusion of MVs.

ACKNOWLEDGMENTS

We thank Catherine Cotter for cells and the NIAID Research and Technologies Branch, Biological Imaging Section, especially Steven Becker, Matthew Gastinger, and Juraj Kabat, for imaging training and data analysis assistance.

This research was supported by the Division of Intramural Research, NIAID, NIH.

REFERENCES

1. **Amegadzie, B. Y., J. R. Sisler, and B. Moss.** 1992. Frame-shift mutations within the vaccinia virus A-type inclusion protein gene. Virology **186:**777–782.
2. **Bisht, H., A. S. Weisberg, P. Szajner, and B. Moss.** 2009. Assembly and disassembly of the capsid-like external scaffold of immature virions during vaccinia virus morphogenesis. J. Virol. **83:**9140–9150.
3. **Cheville, N. F.** 1966. Cytopathologic changes in fowlpox (turkey origin) inclusion body formation. Am. J. Pathol. **49:**723–737.
4. **Ching, Y. C., C. S. Chung, C. Y. Huang, Y. Hsia, Y. L. Tang, and W. Chang.** 2009. Disulfide bond formation at the C termini of vaccinia virus A26 and A27 proteins does not require viral redox enzymes and suppresses glycosaminoglycan-mediated cell fusion. J. Virol. **83:**6464–6476.
5. **Condit, R. C., N. Moussatche, and P. Traktman.** 2006. In a nutshell: structure and assembly of the vaccinia virion. Adv. Virus Res. **66:**31–124.
6. **Downie, A. W.** 1939. A study of the lesions produced experimentally by cowpox virus. J. Pathol. Bacteriol. **48:**361–379.
7. **Earl, P. L., N. Cooper, L. S. Wyatt, B. Moss, and M. W. Carroll.** 1998. Preparation of cell cultures and vaccinia virus stocks, p. 16.16.1–16.16.3. *In* F. M. Ausubel, R. Brent, R. E. Kingston, D. D. Moore, J. G. Seidman, J. A. Smith, and K. Struhl (ed.), Current protocols in molecular biology, vol. 2. John Wiley & Sons, Inc., New York, NY.
8. **Funahashi, S., T. Sato, and H. Shida.** 1988. Cloning and characterization of the gene encoding the major protein of the A-type inclusion body of cowpox virus. J. Gen. Virol. **69:**35–47.

9. **Howard, A. R., T. G. Senkevich, and B. Moss.** 2008. Vaccinia virus A26 and A27 proteins form a stable complex tethered to mature virions by association with the A17 transmembrane protein. J. Virol. **82:**12384–12391.
10. **Ichihashi, Y., and S. Matsumoto.** 1968. The relationship between poxvirus and A-type inclusion body during double infection. Virology **36:**262–270.
11. **Ichihashi, Y., and S. Matsumoto.** 1966. Studies on the nature of Marchal bodies (A-type inclusion) during ectromelia virus infection. Virology **29:**264–275.
12. **Ichihashi, Y., S. Matsumoto, and S. Dales.** 1971. Biogenesis of poxviruses: role of A-type inclusions and host cell membranes in virus dissemination. Virology **46:**507–532.
13. **Knight, J. C., C. S. Goldsmith, A. Tamin, R. L. Regnery, D. C. Regnery, and J. J. Esposito.** 1992. Further analyses of the orthopoxviruses volepox virus and raccoon poxvirus. Virology **190:**423–433.
14. **Marchal, J.** 1930. Infectious ectromelia. A hitherto undescribed virus disease of mice. J. Pathol. Bacteriol. **33:**713–728.
15. **McKelvey, T. A., S. C. Andrews, S. E. Miller, C. A. Ray, and D. J. Pickup.** 2002. Identification of the orthopoxvirus p4c gene, which encodes a structural protein that directs intracellular mature virus particles into A-type inclusions. J. Virol. **76:**11216–11225.
16. **Moss, B., E. N. Rosenblum, E. Katz, and P. M. Grimley.** 1969. Rifampicin: a specific inhibitor of vaccinia virus assembly. Nature **224:**1280–1284.
17. **Nagayama, A., B. G. T. Pogo, and S. Dales.** 1970. Biogenesis of vaccinia: separation of early stages from maturation by means of rifampicin. Virology **40:**1039–1051.
18. **Patel, D. D., D. J. Pickup, and W. K. Joklik.** 1986. Isolation of cowpox virus A-type inclusions and characterization of their major protein component. Virology **149:**174–189.
19. **Rodriguez, D., J. R. Rodriguez, and M. Esteban.** 1993. The vaccinia virus 14-kilodalton fusion protein forms a stable complex with the processed protein encoded by the vaccinia virus A17L gene. J. Virol. **67:**3435–3440.
20. **Shida, H., K. Tanabe, and S. Matsumoto.** 1977. Mechanism of virus occlusion into A-type inclusion during poxvirus infection. Virology **76:**217–233.
21. **Sodeik, B., S. Cudmore, M. Ericsson, M. Esteban, E. G. Niles, and G. Griffiths.** 1995. Assembly of vaccinia virus: incorporation of p14 and p32 into the membrane of the intracellular mature virus. J. Virol. **69:**3560–3574.
22. **Townsley, A., T. G. Senkevich, and B. Moss.** 2005. Vaccinia virus A21 virion membrane protein is required for cell entry and fusion. J. Virol. **79:**9458–9469.
23. **Ulaeto, D., D. Grosenbach, and D. E. Hruby.** 1996. The vaccinia virus 4c and A-type inclusion proteins are specific markers for the intracellular mature virus particle. J. Virol. **70:**3372–3375.
24. **Vazquez, M. I., G. Rivas, D. Cregut, L. Serrano, and M. Esteban.** 1998. The vaccinia virus 14-kilodalton (A27L) fusion protein forms a triple coiled-coil structure and interacts with the 21-kilodalton (A17L) virus membrane protein through a C-terminal alpha-helix. J. Virol. **72:**10126–10137.
25. **Ward, B. M.** 2005. Visualization and characterization of the intracellular movement of vaccinia virus intracellular mature virions. J. Virol. **79:**4755–4763.